HeroMaker: Human-centric Video Editing with Motion Priors

Shiyu Liu
ShanghaiTech University
Shanghai, China
liushy2023@shanghaitech.edu.cn

Zibo Zhao
ShanghaiTech University
Shanghai, China
zhaozb@shanghaitech.edu.cn

Yihao Zhi
The Chinese University of Hong Kong (Shenzhen)
Shenzhen, China
223010099@link.cuhk.edu.cn

Yiqun Zhao
ShanghaiTech University
Shanghai, China
zhaoyq12022@shanghaitech.edu.cn

Binbin Huang
ShanghaiTech University
Shanghai, China
huangbb@shanghaitech.edu.cn

Shuo Wang
ShanghaiTech University
Shanghai, China
wangshuo2022@shanghaitech.edu.cn

Ruoyu Wang
ShanghaiTech University
Shanghai, China
wangry3@shanghaitech.edu.cn

Michael Xuan
UniDT Co. Ltd
Shanghai, China
michael.xuan@unidt.com

Zhengxin Li
ShanghaiTech University
Shanghai, China
lizhx@shanghaitech.edu.cn

Shenghua Gao*
The University of Hong Kong
HKSAR, China
HKU Shanghai Advanced Computing and Intelligent Technology Research Institute
Shanghai, China
gaosh@hku.hk

Abstract

Video generation and editing, particularly human-centric video editing, has seen a surge of interest in its potential to create immersive and dynamic content. A fundamental challenge is ensuring temporal coherence and visual harmony across frames, especially in handling large-scale human motion and maintaining consistency over long sequences. The previous methods, such as zero-shot text-to-video methods with diffusion model, struggle with flickering and length limitations. In contrast, methods employing Video-2D representations grapple with accurately capturing complex structural relationships in large-scale human motion. Simultaneously, some patterns on the human body appear intermittently throughout the video, posing a knotty problem in identifying visual correspondence. To address the above problems, we present HeroMaker. This human-centric video editing framework manipulates the person's appearance within the input video and achieves consistent results across frames. Specifically, we propose to learn the motion priors, which represent the correspondences between dual canonical fields and each video frame, by leveraging the body mesh-based human motion warping and neural deformation-based margin refinement in the video reconstruction framework to ensure the semantic correctness of canonical fields. HeroMaker performs human-centric video editing by manipulating the dual canonical fields and combining them with motion priors to synthesize temporally coherent and visually plausible results. Comprehensive experiments demonstrate that our approach surpasses existing methods regarding temporal consistency, visual quality, and semantic coherence.

CCS Concepts

• **Computing methodologies** → **Computer vision**.

Keywords

Human-centric Video Editing, Diffusion Model, Motion Priors

ACM Reference Format:
Shiyu Liu, Zibo Zhao, Yihao Zhi, Yiqun Zhao, Binbin Huang, Shuo Wang, Ruoyu Wang, Michael Xuan, Zhengxin Li, and Shenghua Gao. 2024. HeroMaker: Human-centric Video Editing with Motion Priors. In *Proceedings of the 32nd ACM International Conference on Multimedia (MM '24), October 28-November 1, 2024, Melbourne, VIC, Australia.* ACM, New York, NY, USA, 10 pages. https://doi.org/10.1145/3664647.3681147

*Corresponding author

MM '24, October 28-November 1, 2024, Melbourne, VIC, Australia

ACM ISBN 979-8-4007-0686-8/24/10
https://doi.org/10.1145/3664647.3681147

1 Introduction

Human-centric video editing focuses on modifying the individual within a given video and generating temporally coherent results. This technique has numerous potential applications, such as media

content production, virtual reality, and video games. A pivotal challenge in human-centric video editing is maintaining coherence and harmonious results across frames when people can move freely in the video.

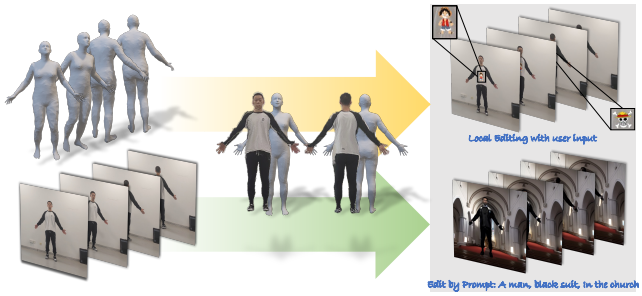

(a) Human Mesh acquisition (b) Dual Canonical Fields Learning (c) Diverse Video Editing

Figure 1: We present HeroMaker, a new video representation with motion priors for human-centric video editing, which contains human motion warping, margin refinements, and dual canonical fields. As illustrated in (a), our model employs the body mesh to portray the structure information of people in the video. From (a) to (b), our model reconstructs the video with explicit human motion warping and neural margin refinements between dual canonical fields and each video frame. (c) shows the two edited results from HeroMaker, which are temporally consistent and plausible.

Recent zero-shot text-to-video methods explore extracting and incorporating various structural correspondences using infer-frame attention maps [6, 8, 32, 55], optical flows [11, 58], and nn-fields [19]. Although the temporal consistency has improved, they still struggle with flickering and length limitations. Alternatively, some researchers have explored video-2D representations, storing the video information in atlases [30] or canonical images [46] to propagate changes over time. However, they grapple with accurately capturing complex structural relationships in large-scale human motion. Moreover, many studies have focused on reconstructing a human body in 3D and attempting to edit it [38, 51]. While promising, these methods often present challenges regarding cost or unfriendly user-controlled environments due to the semantic-less texture maps and the long-term optimization needs.

Since each human part is unique, patterns on the human body appear intermittently throughout the video due to self-occlusion, posing a knotty problem in identifying correspondence to ensure consistent video editing. As a video-2D representation method, CoDeF[46] builds correspondences by learning a neural deformation field from a canonical image to each frame and edits the canonical image to enhance the consistency. Although it achieves high-fidelity reconstruction, the canonical image differs from natural images. This makes it challenging to use editing tools like ControlNet [62] to generate semantically plausible results.

Given CoDeF's success, we leverage the human body mesh to obtain semantic human canonical images, capturing structural and texture correspondences. Our framework defines motion priors, incorporating human motion warping, neural margin refinements, and dual canonical fields to achieve this goal. First, we employ an off-the-shelf human mesh estimator to set up an initial body mesh. We then refine this mesh in a two-step optimization to match the person's shape in videos to ensure more accurate motion priors. Resorting to motion priors, our model defines the dual canonical fields with a frontal and back body mesh under A-pose to obtain the vast majority of human body details. It reconstructs the video with explicit human motion warping and neural margin refinements between dual canonical fields and each human-centric video frame. Our model performs human-centric video editing by manipulating the semantic-aware dual canonical fields. Additionally, it supports diverse user interactions for modifying the videos and synthesizes temporally coherent and visually plausible results.

We summarize our contributions as follows:

- We propose a new human-centric video representation combining motion priors and deformation fields to reconstruct and edit the video.
- We leverage the motion priors with human motion warping based on body mesh, neural margin refinements, and dual canonical fields to identify accurate structural correspondence and produce coherent results.
- Extensive experiments demonstrate that our model could produce temporal coherent and plausible results, especially during large-scale human motion.

2 Related Work

2.1 Text-to-Video Generation and Editing.

Recent works attempt to extend the diffusion model into a T2V editing model [2, 5, 6, 15–17, 19, 21, 22, 24, 25, 27, 32, 35, 36, 39, 42, 44, 48, 49, 52, 55, 56, 59–61, 65]. Tune-A-Video [55] and Control-A-Video [8] extend a diffusion model to the spatial-temporal domain and fine-tune it with source videos. However, those models struggle with complex motions and long sequences. Text2Video-Zero [32] and ControlVideo [64] use ControlNet [62] to preserve the per-frame structure but face challenges with temporal consistency. FateZero [48] and vid2vid-zero [53] employ attention maps for shape-aware editing based on prompt-to-prompt [23], yet temporal issues persist. Rerender-A-Video [58], TokenFlow [19], and VideoControlNet [27] use optical flow to manage inter-frame relationships, enhancing consistency. Despite this, they encounter difficulties with large-scale human motion. TokenFlow [19] enforces linear combinations between diffusion features based on source correspondences, but the pre-defined combination weights are not universally applicable, causing high-frequency flickering.

These methods focus on augmenting inter-frame attention modeling with diffusion models to preserve spatial structure, but temporal consistency challenges remain. Recently, AnimateDiff [21] introduced a motion module trained on extensive video data without fine-tuning the diffusion model, improving temporal consistency. Furthermore, human-centric videos have further explored some works [26, 57, 67] and achieved visually plausible results, but generating similar effects with limited video data remains challenging. In contrast, our method effectively leverages human motion priors for text-guided video editing.

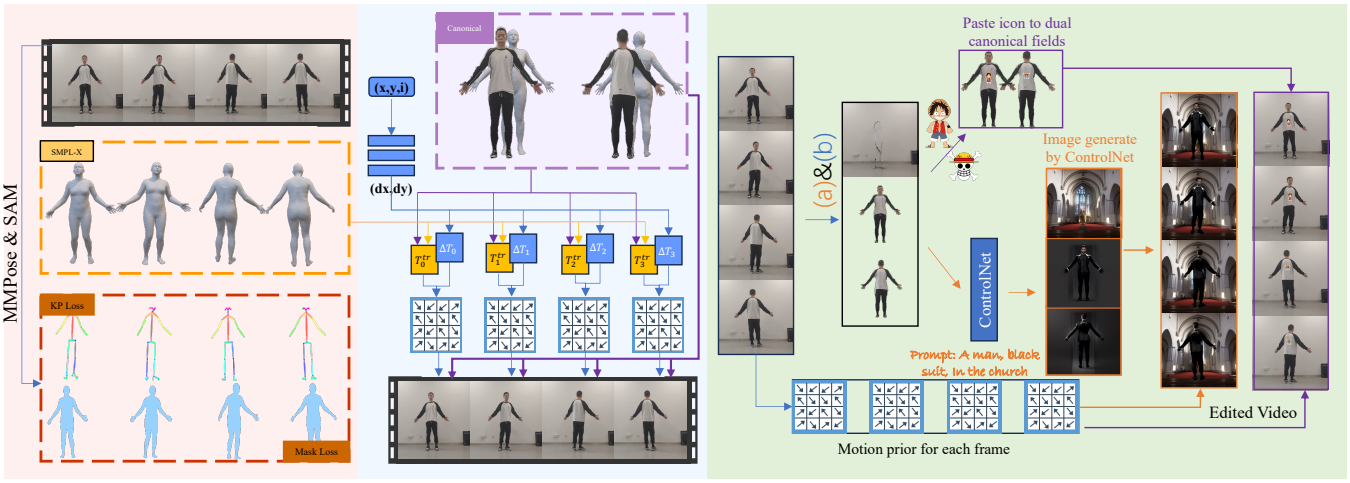

Figure 2: We propose a multi-stage framework for human-centric video editing. We first acquire the motion priors for each frame based on SMPL-X [47] (a). Building upon the motion priors, we devise an editing-friendly video representation to reconstruct the input video (b). Then, our optimized video representation enables superior editing performance as in (c).

2.2 Temporal Propagation in video editing.

Another important aspect of video editing involves using a strong video representation. VideoSnap [66] compresses viudeos by converting them into one or several images using spatial and temporal features, then trains a network to transform these images back into videos. The layered neural atlas breaks down the video into layers, mapping the subject and background of all frames using 2D UV maps for editing. Once the atlas is created, edits can be made on keyframes or directly on the atlas, with changes automatically applying to all frames [4, 7, 13, 28, 33]. CoDeF [46] combines 3D deformation fields with a 2D hash-based image to enhance video representation. However, Video Snapshot [66], the atlas [30], and canonical images [46] all use optical flow to predict relationships between frames. They struggle with reconstructing and editing videos with large-scale human motion, leading to mismatched details and unnatural results.

2.3 3D Human Reconstruction and Editing

3D human reconstruction and editing are closely related to human-centric video editing tasks. Many studies focus on accurately reconstructing a human body and texture using the SMPL+D model [1, 18] or implicit functions [20, 29, 54] from monocular videos. Nevertheless, these studies aim to create and drive precise human models, often overlooking editing ease and user-friendliness. Some methods like SINE [3] and SKED [43] allow local region editing in 3D, while Dyn-E [63] and Control4D [51] enable editing dynamic content. However, Dyn-E is limited to local appearance changes by the user, and Control4D [51] requires multi-view videos and can only handle short videos with minimal motion. Recently, DynVideo-E [38] has tried 3D editing of monocular videos using text, but it is not user-friendly as the process can take tens of hours. Although these methods can produce high-fidelity results, their cost, size, and controlled environment are unfriendly to users. Video or image editing frameworks tend to avoid these issues. Our approach uses motion priors for the human body and converts them into pixel position relationships between frames, transforming the task into 2D image editing while maintaining 3D structure accuracy. It is a crucial motivation behind our work, which aims to introduce a new human-centric video representation to address image and video editing challenges. We do not compare our method with others as some recent works [38, 51, 63] are not open-source.

3 Method

Given a human-centric video, we aim to modify its visual attributes based on diverse user interactions while maintaining correct structural correspondence and temporal consistency. We tackle this problem with a multi-stage framework, namely reconstructing and editing. As shown in Fig.2, HeroMaker introduces a novel video representation by leveraging motion priors based on the SMPL-X [47], which establishes the transformation correspondence from the canonical field to each video frame. In the following, we illustrate motion priors in Sec.3.1, describe our novel video representation in Sec.3.2, and finally detail the editing process and applications of the entire framework in Sec.3.3.

3.1 Preliminary: Motion Priors

As mentioned earlier, the visual quality of video editing greatly depends on the established video representation. To improve this representation and make video editing easier, we resort to readily accessible motion priors. Specifically, we mitigate the deformation ambiguity by dividing it into two parts: explicit human motion warping and neural margin refinements. Thus, our first step is to obtain reliable motion priors.

As depicted in Fig.2 (a), starting with a human-centric video $\{I_i\}_{i=0}^{N-1}$ consisting of N frames, we apply the off-the-shelf OSX [37] to predict camera parameters P_i and SMPL-X [47] coefficients due to

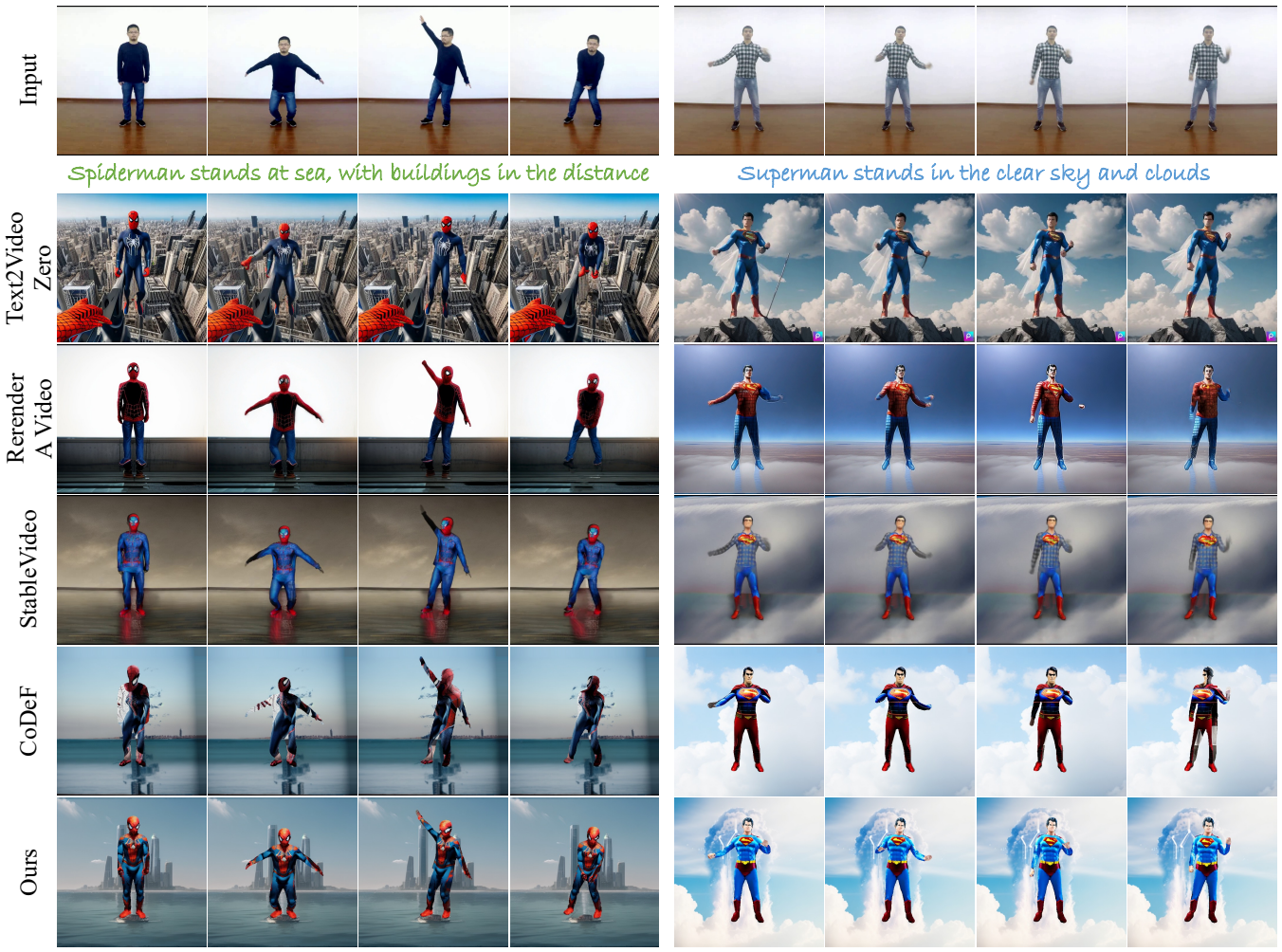

Figure 3: Qualitative analysis of video editing by the prompt. We compare our method against baselines using prompts. The first row is the input video, and the colorful description is the editing prompt. Text2VideoZero and Rerender-A-Video suffer from self-occlusion and large-scale movements, thus producing temporal inconsistent results. StableVideo struggles with complex structures, resulting in decreased fidelity of the edited results. CoDeF's canonical images differ from the natural ones, leading to results lacking semantics. The results of our method, in the last row, are temporally coherent and plausible.

its robustness toward partial observations and high efficiency. The SMPL-X [47] is a differentiable function $S(\beta, \theta, \psi) \rightarrow (V, F)$ that outputs a 3D human body mesh with 10475 vertices $V \in \mathbb{R}^{10475\times3}$ and 20908 faces $F \in \mathbb{R}^{20908\times3}$, where $\psi \in \mathbb{R}^{10}$ is the facial expression parameters, $\beta \in \mathbb{R}^{10}$ and $\theta \in \mathbb{R}^{22\times3}$ are the body shape parameters and pose parameters, respectively. To improve the accuracy of the transformation correspondences, we adopt a two-step optimization strategy to achieve a more accurate SMPL-X [47] fit, instead of relying directly on the regression-based estimates from OSX [37].

Firstly, we refine the SMPL-X coefficients with 2d keypoints. Specifically, we leverage mmpose [12] to attain 2D keypoints $P_{i(2D)}$ for each frame i. We optimize over the learnable parameters $\theta_{i=0}^{N-1}$ by minimizing the difference between estimated 2D keypoints $P_{i(2D)}$ and corresponding projected 2D joints $P_i(J_{\text{sub}})$, where P_i is the projection matrix. Additionally, we employ a temporal regularization $\mathcal{L}^1_{\text{reg}}$ on output mesh vertices V^i_m to ensure continuity. The optimization objective of the first stage is:

$$\mathcal{L}^1 = \mathcal{L}_{\text{kps}} + \lambda^1_{\text{reg}}\mathcal{L}^1_{\text{reg}} \tag{1}$$

$$\mathcal{L}_{\text{kps}} = \|P_{i(2D)} - P_i(J_{\text{sub}})\|_2^2 \tag{2}$$

$$\mathcal{L}^1_{\text{reg}} = \|V_m^{[0:n-2]} - V_m^{[1:n-1]}\|_2^2 \tag{3}$$

To further improve the flexibility of the SMPL-X [47] model's expression ability, making it able to match the clothed human better in the video, rather than a skinned person. In the second stage, we added a per-vertex offset $D \in \mathbb{R}^{10475\times3}$, to capture the details of each frame and define the model as:

$$S(\beta, \theta, \psi, D) = \text{LBS}(T(\beta, \theta, \psi, D), J(\beta), \theta, W) \tag{4}$$

$$T(\beta, \theta, \psi, D) = T + B_s(\beta) + B_p(\theta) + B_e(\psi) + D \tag{5}$$

where T is a mean shape template, B_s, B_p and B_e are shape, pose and expression blend shapes, respectively. LBS denotes linear blending skinning and W is the vertices' skinning weights. We only optimize D in this stage to avoid overfitting. Since we expect the rendered human outline to align with the foreground mask, we utilize mask loss as a supervision. We use SAM-Track [10] to get a per-frame binary mask M_i of human and minimize the difference between the silhouette of the rendered body $R^s(P_i, \{V_i, F\})$ and the obtained mask M_i, where R^s denotes the differentiable silhouette rasterizer. To ensure mesh smoothness, we regulate the offset with Laplacian smoothing loss [14, 45] $L_{\text{Laplacian}}$ and L_2 regularization. The optimization objective of the second stage is:

$$\mathcal{L}^2 = \mathcal{L}_{\text{silhouette}} + \lambda^2_{\text{reg}}\mathcal{L}^2_{\text{reg}} \tag{6}$$

$$\mathcal{L}_{\text{silhouette}} = \|R^s(P, \{V_i, F\}) - M_i\|^2_2 \tag{7}$$

$$\mathcal{L}^2_{\text{reg}} = L_{\text{Laplacian}}(D) + \gamma\|D\|^2_2 \tag{8}$$

Finally, we acquire sufficiently expressive motion priors.

3.2 Video Reconstruction with Motion Priors

We find the strong video representation that maintains better temporal continuity compared to the inter-frame attention model. Intuitively, the prerequisite for promising editing is establishing a meaningful canonical field. Meanwhile, a well-defined deformation field can relieve the ambiguity in the canonical field, subsequently benefiting high-quality editing outcomes. Using motion priors described in Sec. 3.1, we aim to create a more user-friendly video representation. This approach can effectively transform human-centric video editing issues into image editing tasks.

Previous video representation methods can be mainly grouped into two typesThe first [30] uses a UV mapping between pixel space and atlas, but semantic-less atlas makes editing complex. The second [46] tries to compress video content into images, but finding the correspondence when dealing with large-scale human motion is challenging. Thus, we devise dual canonical fields and decompose the temporal deformation based on motion priors. As shown in Fig.2, our video representation comprised of three components:

Dual canonical fields. We define the canonical human body as the A-posed SMPL-X+D, *i.e.* $S_c = S(\bar{\beta}, \theta_A, \bar{\psi}) + \bar{D}$ with mean estimated coefficients across video frames. Specifically, we adopt a dual canonical fields design in which we choose the front view C_{front} and back view C_{back} of the canonical human body for information complementarity. As for the network structure, our dual canonical fields are constructed using two 2D multi-resolution hash encodings, which map a 2D position (x, y) to (R, G, B) color.

Explicit Human motion warping. To alleviate the issue of overfitting resulting from directly learning a deformation field [46], we expect that explicit human motion warping dominates the overall deformation, while neural deformation serves as a refinement. Human motion warping is parametric-free, yet it provides semantic correspondences across frames in video representation.

Inspired by Liquid Warping GAN [40, 41], we build human motion warping using the Neural Mesh Renderer (NMR) [31]. To reconstruct a target frame I_i, we first query the canonical fields to acquire two canonical images I_{front} and I_{back}, and then we embed them into texture space using a weak-perspective camera as S_c. Since our motion priors are topologically consistent, we can easily obtain the transformation $T^{\text{tr}}_{\text{front}}$ and $T^{\text{tr}}_{\text{back}}$, which warps the information from the canonical fields to the target frame. Moreover, we compute a mask to fuse information from C_{front} and C_{back}. For more details, please refer to the supplementary materials. In simpler terms, we define the deformation in a canonical-to-observation direction, which naturally prevents the drawback of backward deformation [9].

Neural Margin refinement. Now, we can make approximate transformations with human motion warping. However, human motion warping only deals with rigid transform. It can't handle detailed clothes and fine-grained non-rigid deformations. In other words, the information in the position $I_i(x, y)$ is not solely determined by the transformation $T^{tr}_{front|back}$. To address this, we design a small refinement field and padding strategy to improve the margin part of humans in videos.

For the refinement filed, we want to further reduce the error by learning a small positional offset. Specifically, we feed in a triplet (x, y, i) into the refinement field and produce small offset $\Delta T : (\Delta x, \Delta y)$. The overall transformation from front or back canonical image to each target frame is represented as $T = T^{\text{tr}}_{\text{front|back}} + \Delta T$, where $T^{\text{tr}}_{\text{front|back}}$ is obtained based on human motion warping.

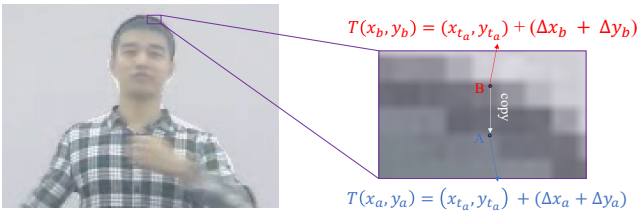

Figure 4: Margin refine method. Our method deals with the transformation relationships of points outside the mesh transformation matrix region and inside the human mask.

As shown in Fig. 4, the final transformation combines human motion warping and margin refinement. The human mask M and the region affected by human warping do not entirely overlap. Hence, the final transformation is divided into two parts. For a position where the transformation $T^{tr}_{front|back}$ is applicable, we get the final transformation T_{in} by combining the current position transformation with a slight refinement. For positions outside the transformation but within the human mask M, we use the transformation from the nearest position within $T_{front|back(nearest-in)}$ and add a slight refinement to get the final transformation T_{out}.

$$T_{in} = T^{tr}_{front|back(in)} + \Delta T_{in} \tag{9}$$

$$T_{out} = T^{tr}_{front|back(nearest-in)} + \Delta T_{out} \tag{10}$$

We select the two frames $I_{\text{nn\_front}}, I_{\text{nn\_back}}$ from the video closest to the front-view and back-view as regularization for training. Specifically, we additionally reconstruct the target frame $\hat{I}_i$ with the information from $I_{\text{nn\_front}}$ or $I_{\text{nn\_back}}$ according to the orientation similarity of the pelvis. In this way, we can largely preserve the semantic information.

Our representation is jointly trained by minimizing the reconstruction loss L_{rec} between the predicted image $\hat{I}$ and the original one I using mean square error. Moreover, we constrain the output

of the deform field using L_2 norm empirically. Overall, the loss function of video reconstruction with motion priors can be written as:

$$\mathcal{L}^3 = \mathcal{L}_{\text{rec}}(\hat{I}_i, I_i) + \lambda_{\text{deform}}\|\Delta T\|_2^2 + \lambda^3_{\text{reg}}\mathcal{L}^3_{\text{reg}} \tag{11}$$

$$\mathcal{L}^3_{\text{reg}} = \sum_{I_i \in \text{front}} L_{\text{rec}}(\hat{I_i'}, I_i) + \sum_{I_i \in \text{back}} L_{\text{rec}}(\hat{I_i'}, I_i) \tag{12}$$

3.3 Video Editing Module

Upon the optimized video representation, we can obtain the trained front canonical image I_{front} and back canonical image I_{back} by querying the C_{front} and C_{back} with position (x, y). Our dual canonical fields design retains semantic and structural information but introduce a new challenge in terms of semantic consistency. Editing the two images separately using ControlNet [62] may yield inharmonious results due to randomness during the diffusing and denoising process. We suggest resolving this issue through a simple yet effective strategy to ensure editing coherence. Specifically, we concatenate the I_{front} and I_{back} along the width axis before using ControlNet [27]. The self-attention mechanism implicitly builds the correlation between the two images.

As shown in Fig.2 (c), we explore two different editing scenes: 1) **Video editing by prompt**. Users could modify the content of the human and background separately using text inputs. 2) **Video editing with user input**. Users could directly draw on the canonical images as they wish. For example, they can attach a logo to clothes and automatically propagate it throughout the video. Moreover, HeroMaker supports editing a person individually within a video with multiple people, which differs from most competing methods.

4 Experiments

4.1 Experimental Setup

Implementation Details. HeroMaker is implemented in PyTorch. In the first stage, we optimize the mesh with the Adam optimizer(lr = 0.0001, $\beta = (0.9, 0.99)$) for 200 iterations. The regularization parameter, denoted as $\lambda^1_{reg} = 0.2$. In the second stage, We optimize for 20 iterations per frame with a learning rate of 0.0005, $\lambda^2_{reg} = 0.2$ and $\gamma = 10$. During video reconstruction, we jointly train dual canonical fields and neural margin refinement field together with the Adam optimizer(lr=0.0001, $\beta = (\mathbf{0.9}, \mathbf{0.99})$) for 15000 iterations. We employ the Stable Diffusion v1.5 model, and ControlNet [62] provides structure guidance regarding edges. For image editing, we implement 30 timesteps for DDIM sampling.

Dataset. We validate the effectiveness of our full pipeline using two datasets, including selected videos from the iPER [40, 41] and in-the-wild internet videos. These videos encompass individuals with diverse body shapes, each performing with different speeds and amplitudes. All videos consist of 50 to 200 frames, and we employ $2 \sim 4$ prompts during editing.

Baselines. For video editing by prompts, we compare our model with Text2Video-Zero [32], Rerender-A-Video [58], StableVideo [7] and CoDeF [46] to show the temporal consistency and ability to match the prompts. We compare our method with NLA [30] and CoDeF [46] in video editing with the user input to validate the ability to represent the video in a structure-aware correspondence.

Method	$E_{\text{vertices}} \downarrow$	CLIP↑
Text2Video-Zero [32]	27.61	25.00
Rerender-A-Video [58]	25.85	26.05
StableVideo[7]	10.53	26.43
CoDeF [46]	26.22	27.48
Ours	**7.81**	**27.70**

Table 1: Quantitative comparison on prompt-based video editing. We estimate and compute the average mesh vertices error as E_{vertices} in the original and edited videos. For textual alignment, we report the average CLIP [50] score.

Method	Textual fidelity consistency ↑	Shape preservation↑	Visual effect↑
Text2Video-Zero [32]	0.531	0.500	0.469
Rerender-A-Video [58]	0.594	0.438	0.563
StableVideo[7]	0.375	0.500	0.469
CoDeF [46]	0.375	0.344	0.344
Ours	**0.813**	**0.625**	**0.625**

Table 2: User study on prompt-based video editing.

Method	NLA [30]	CoDeF [46]	Ours
Visual effect ↑	0.375	0.365	**0.750**

Table 3: User study on user interactive video editing.

Evaluation Metrics. Human-centric video editing aims to reflect the editing prompt accurately while maintaining original shape coherency and temporal consistency. To measure shape coherency, we estimate the human mesh in the original and edited video using OSX [37] and compute the average error in mesh vertices as E_{vertices}. For textual alignment, we use CLIP [50] score, which calculates how similar the prompt's description is to each frame in the edited video. However, these metrics alone do not fully represent the visual quality of edited videos. Thus, we conduct a user study. Participants are shown descriptions and edited results from different methods and asked to rate three aspects: textual fidelity with temporal continuity, shape preservation, and visual effect.

4.2 Comparison with Baselines

Quantitative Comparison. Following previous works, we evaluate our method and baselines with different metrics. As indicated in Table. 1, our method surpasses previous works in all metrics, demonstrating that our edited results align closely with the prompts and maintain the original body shape. We further conduct user studies as described in Sec.4.1. As shown in Table. 2 and Table. 3, the participants exhibit a clear preference for our results.

Qualitative Comparison. Fig.3 shows the visual results of prompt-based video editing. Text2Video-Zero [32] and Rerender-A-Video [58] generate outputs semantically aligned with the text description but fail to maintain temporal consistency. For instance, the body shapes are flickering, and the arms are distorted (see Spider-Man and Superman in Fig. 3). StableVideo [7] exhibits satisfactory temporal

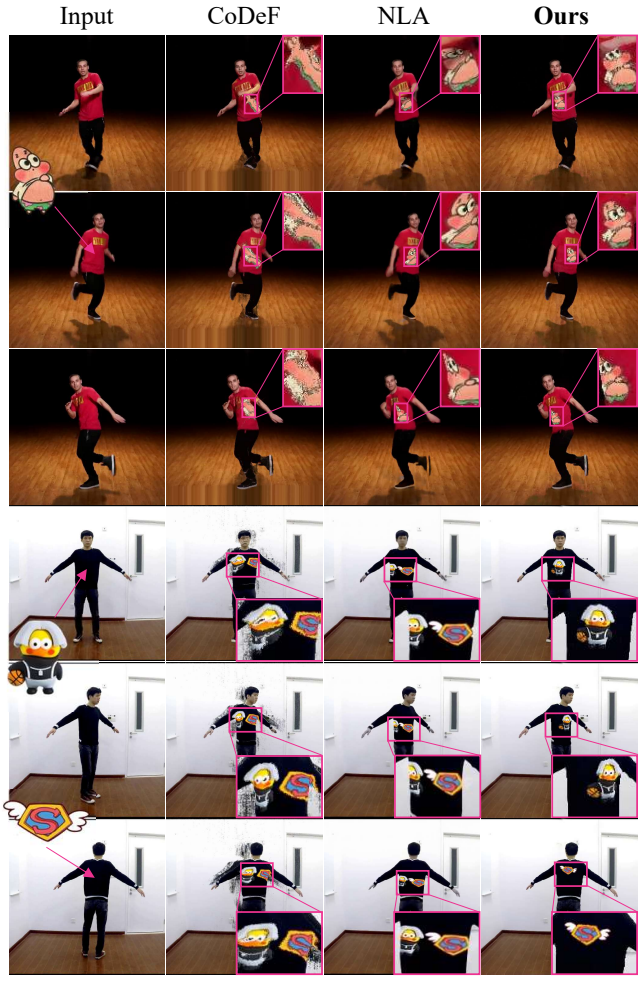

Figure 5: Qualitative analysis of video editing with user input. Our method supports local editing and allows users to add customized icons accurately to the region of interest. We compare our method against NLA [30] and CoDeF [46].

consistency. However, it is prone to generating outputs with reduced fidelity. Since CoDeF [46] learns the deformation field and the canonical image without structure information, it generates different results from natural images when handling human-centric videos. According to Fig. 3, leveraging the motion priors achieves temporal consistency while preserving fidelity successfully.

Furthermore, representing the video with motion priors allows our model to edit the human body locally. It enables users to edit regions of interest while maintaining the other parts. In Fig. 5, we compare our method to NLA [30] and CoDeF [46] in user interactive video editing. NLA [30] and CoDeF [46] models use optical flow to maintain the correspondence between frames. However, estimating optical flow for complex human motion is difficult, which leads to visual flaws. Although NLA [30] shows good textured results, it fails to maintain geometry consistency between human motion. CoDeF [46] leads to information losses when encoding the video into a canonical content field. In some cases, the correspondence of body deformation deviates, causing unpleasant edited results. In contrast, our model utilizes motion priors and thus learns human-aware canonical fields, ensuring that the edited contents are attached to the appropriate positions.

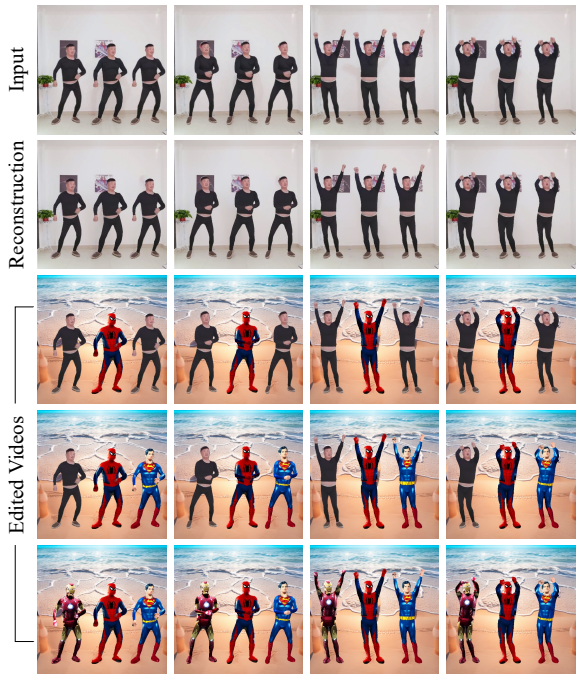

Figure 6: Multiple people edited results. Our method can be extended to reconstruct and edit videos with multiple people present. In the subsequent stage, users can edit the person in the scene individually, providing greater flexibility.

Additionally, unlike most previous methods, HeroMaker offers the ability to easily modify any character within a video containing multiple people, as illustrated in Fig. 6. This capability enhances the appeal and flexibility of human-centric video editing, providing users with a unique and engaging experience.

4.3 Ablation Studies

To verify the contributions of different modules to overall performance, we systematically deactivate specific modules in our framework and present the visual comparison in Fig.7. In this section, we analyze the impact of varying degrees of SMPL-X refinement, the addition of a deform module, and the necessity of learning canonical fields. We define method (a) as the model without SMPL-X refinement and the neural deformation module. Method (b) incorporates the neural deformation module into the baseline. Since our framework performs SMPL-X refinement in two stages, method (c) applies only the first refinement stage, whereas method (d) represents our full model.

Neural deformation module. The neural deformation module aims to correct estimation errors from the SMPL-X network by ensuring the alignment of frame images with the canonical fields

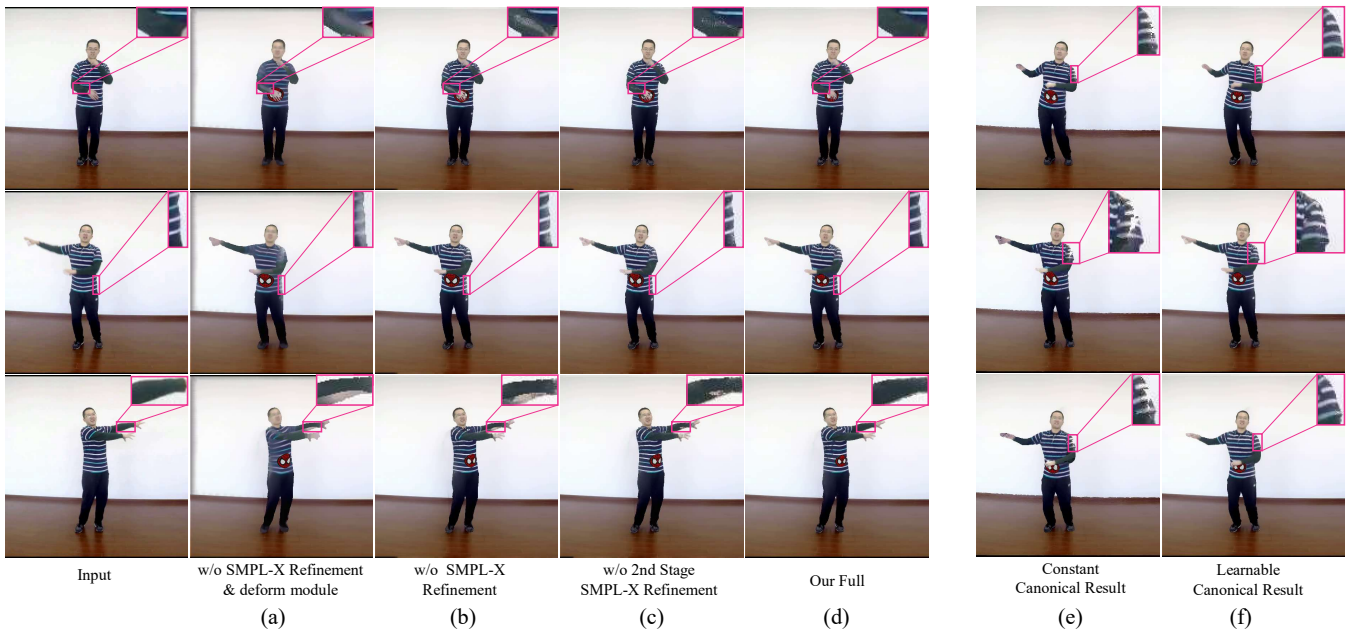

Figure 7: Qualitative ablation results. Compared to method (a), method (b) benefits from a neural deformation module to correct estimation errors from the SMPL-X network. The method (c) further improves the results using first-stage SMPL-X refinement, effectively improving motion priors. Our entire uses a neural deformation module and two stages of SMPL-X refinement to achieve precise mesh deformation. Additionally, we demonstrate the necessity of learnable canonical fields by comparing method (e) versus method (f).

under motion priors. Comparing methods (a) and (b) shows that this module improves image clarity and reduces edge deviations, proving its effectiveness in improving visual quality by learning precise correspondences.

SMPL-X refinement. The refinement process reduces mesh deviations identified by the SMPL-X network and utilizes 2D keypoints and inter-frame mesh deviations for optimization in the first stage. The improved image quality in method (c) shows that correct motion priors positively affect the result. In the second refinement state, edge artifacts are further corrected, highlighting the importance of refinement in achieving accurate mesh deformation.

Learnable canonical fields. Additionally, to demonstrate the necessity of learnable canonical fields, we select the two images closest to the front and back view as canonical images and then optimize the deformation network to obtain the final results. This approach extracts as much information as possible from the video while ensuring semantic information. However, as shown in Fig. 7, comparing method (e) with method (f) demonstrates that learnable canonical fields capture more detailed and relevant information from video sequences, thereby reducing reconstruction errors and improving edge definition. Constant canonical images, despite their simplicity, fail to accommodate the complexity and randomness of motion, leading to artifacts in reconstructed images.

4.4 Discussion

Extensive experiments demonstrate that our HeroMaker framework can edit human-centric videos, producing temporally coherent and visually plausible results. Specifically, our method utilizes a parametric 3D body model to obtain motion priors. Moreover, we added a learnable offset to capture the details of each frame. However, the distribution of vertices on the body's surface is sparse. For loose and complex clothing, like dresses, the body mesh expands outward to fit the structural correspondences, but this limited flexibility makes it challenging to achieve accurate correspondences. A possible solution is to introduce an adaptive upsampling technique [34] on the triangles that can make motion priors more expressive, thereby better handling dress cases.

5 Conclusion

In this paper, we present HeroMaker, an innovative framework that prioritizes human-centric video editing. Our approach utilizes motion priors based on human body mesh to establish the transformation correspondences from human-aware canonical fields to each video frame. Powered by our devised video representation, we maintain meaningful and structural canonical fields, enabling the subsequent synthesis of temporally coherent and plausible results in response to diverse user interactions. Extensive experiments and visual results demonstrate the superior performance of HeroMaker, while ablation studies confirm the effectiveness of our design.

Acknowledgments

The work was supported by NSFC #62172279, NSFC #61932020, and Program of Shanghai Academic Research Leader.

References

[1] Thiemo Alldieck, Marcus Magnor, Weipeng Xu, Christian Theobalt, and Gerard Pons-Moll. 2018. Video Based Reconstruction of 3D People Models. In *IEEE Conference on Computer Vision and Pattern Recognition*.

[2] Omri Avrahami, Ohad Fried, and Dani Lischinski. 2022. Blended Latent Diffusion. *arXiv preprint arXiv:2206.02779* (2022). arXiv:2206.02779.

[3] Chong Bao, Yinda Zhang, Bangbang Yang, Tianxing Fan, Zesong Yang, Hujun Bao, Guofeng Zhang, and Zhaopeng Cui. 2023. SINE: Semantic-driven Image-based NeRF Editing with Prior-guided Editing Field. In *The IEEE/CVF Computer Vision and Pattern Recognition Conference (CVPR)*.

[4] Omer Bar-Tal, Dolev Ofri-Amar, Rafail Fridman, Yoni Kasten, and Tali Dekel. 2022. Text2live: Text-driven layered image and video editing. In *European Conference on Computer Vision*. Springer, 707–723.

[5] Andreas Blattmann, Robin Rombach, Huan Ling, Tim Dockhorn, Seung Wook Kim, Sanja Fidler, and Karsten Kreis. 2023. Align your Latents: High-Resolution Video Synthesis with Latent Diffusion Models. arXiv:2304.08818 [cs.CV]

[6] Duygu Ceylan, Chun-Hao Paul Huang, and Niloy J Mitra. 2023. Pix2Video: Video Editing using Image Diffusion. In *Proceedings of the International Conference on Computer Vision (ICCV)*.

[7] Wenhao Chai, Xun Guo, Gaoang Wang, and Yan Lu. 2023. StableVideo: Text-driven Consistency-aware Diffusion Video Editing. *arXiv preprint arXiv:2308.09592* (2023).

[8] Weifeng Chen, Jie Wu, Pan Xie, Hefeng Wu, Jiashi Li, Xin Xia, Xuefeng Xiao, and Liang Lin. 2023. Control-A-Video: Controllable Text-to-Video Generation with Diffusion Models. arXiv:2305.13840 [cs.CV]

[9] Xu Chen, Yufeng Zheng, Michael J. Black, Otmar Hilliges, and Andreas Geiger. 2021. SNARF: Differentiable Forward Skinning for Animating Non-Rigid Neural Implicit Shapes. In *Proceedings of the IEEE/CVF International Conference on Computer Vision (ICCV)*. 11594–11604.

[10] Yangming Cheng, Liulei Li, Yuanyou Xu, Xiaodi Li, Zongxin Yang, Wenguan Wang, and Yi Yang. 2023. Segment and Track Anything. *arXiv preprint arXiv:2305.06558* (2023).

[11] Yuren Cong, Mengmeng Xu, Christian Simon, Shoufa Chen, Jiawei Ren, Yanping Xie, Juan-Manuel Perez-Rua, Bodo Rosenhahn, Tao Xiang, and Sen He. 2023. FLATTEN: Optical Flow-guided ATTENtion for Consistent Text-to-Video Editing. In *Proceedings of the International Conference on Computer Vision (ICCV)*.

[12] MMPose Contributors. 2020. OpenMMLab Pose Estimation Toolbox and Benchmark. https://github.com/open-mmlab/mmpose.

[13] Paul Couairon, Clément Rambour, Jean-Emmanuel Haugeard, and Nicolas Thome. 2023. VidEdit: Zero-Shot and Spatially Aware Text-Driven Video Editing. arXiv:2306.08707 [cs.CV]

[14] Mathieu Desbrun, Mark Meyer, Peter Schröder, and Alan H. Barr. 1999. Implicit Fairing of Irregular Meshes using Diffusion and Curvature Flow. In *SIGGRAPH*.

[15] Zhongjie Duan, Lizhou You, Chengyu Wang, Cen Chen, Ziheng Wu, Weining Qian, and Jun Huang. 2023. DiffSynth: Latent In-Iteration Deflickering for Realistic Video Synthesis. arXiv:2308.03463 [cs.CV]

[16] Patrick Esser, Johnathan Chiu, Parmida Atighehchian, Jonathan Granskog, and Anastasis Germanidis. 2023. Structure and Content-Guided Video Synthesis with Diffusion Models. arXiv:2302.03011 [cs.CV]

[17] Ruoyu Feng, Wenming Weng, Yanhui Wang, Yuhui Yuan, Jianmin Bao, Chong Luo, Zhibo Chen, and Baining Guo. 2023. CCEdit: Creative and Controllable Video Editing via Diffusion Models. arXiv:2309.16496 [cs.CV]

[18] Yao Feng, Jinlong Yang, Marc Pollefeys, Michael J. Black, and Timo Bolkart. 2022. Capturing and Animation of Body and Clothing from Monocular Video. In *SIGGRAPH Asia 2022 Conference Papers* (Daegu, Republic of Korea) *(SA '22)*. Article 45, 9 pages.

[19] Michal Geyer, Omer Bar-Tal, Shai Bagon, and Tali Dekel. 2023. TokenFlow: Consistent Diffusion Features for Consistent Video Editing. *arXiv preprint arxiv:2307.10373* (2023).

[20] Chen Guo, Tianjian Jiang, Xu Chen, Jie Song, and Otmar Hilliges. 2023. Vid2Avatar: 3D Avatar Reconstruction from Videos in the Wild via Self-supervised Scene Decomposition. In *Proceedings of the IEEE/CVF Conference on Computer Vision and Pattern Recognition (CVPR)*.

[21] Yuwei Guo, Ceyuan Yang, Anyi Rao, Zhengyang Liang, Yaohui Wang, Yu Qiao, Maneesh Agrawala, Dahua Lin, and Bo Dai. 2024. AnimateDiff: Animate Your Personalized Text-to-Image Diffusion Models without Specific Tuning. *International Conference on Learning Representations* (2024).

[22] Yingqing He, Menghan Xia, Haoxin Chen, Xiaodong Cun, Yuan Gong, Jinbo Xing, Yong Zhang, Xintao Wang, Chao Weng, Ying Shan, and Qifeng Chen. 2023. Animate-A-Story: Storytelling with Retrieval-Augmented Video Generation. arXiv:2307.06940 [cs.CV]

[23] Amir Hertz, Ron Mokady, Jay Tenenbaum, Kfir Aberman, Yael Pritch, and Daniel Cohen-Or. 2022. Prompt-to-Prompt Image Editing with Cross Attention Control. *arXiv preprint arXiv:2208.01626* (2022).

[24] Jonathan Ho, William Chan, Chitwan Saharia, Jay Whang, Ruiqi Gao, Alexey Gritsenko, Diederik P. Kingma, Ben Poole, Mohammad Norouzi, David J. Fleet, and Tim Salimans. 2022. Imagen Video: High Definition Video Generation with Diffusion Models. arXiv:2210.02303 [cs.CV]

[25] Jonathan Ho, Tim Salimans, Alexey Gritsenko, William Chan, Mohammad Norouzi, and David J Fleet. 2022. Video diffusion models. *arXiv:2204.03458* (2022).

[26] Li Hu, Xin Gao, Peng Zhang, Ke Sun, Bang Zhang, and Liefeng Bo. 2023. Animate Anyone: Consistent and Controllable Image-to-Video Synthesis for Character Animation. *arXiv preprint arXiv:2311.17117* (2023).

[27] Zhihao Hu and Dong Xu. 2023. VideoControlNet: A Motion-Guided Video-to-Video Translation Framework by Using Diffusion Model with ControlNet. arXiv:2307.14073 [cs.CV]

[28] Jiahui Huang, Leonid Sigal, Kwang Moo Yi, Oliver Wang, and Joon-Young Lee. 2023. INVE: Interactive Neural Video Editing. arXiv:2307.07663 [cs.CV]

[29] Boyi Jiang, Yang Hong, Hujun Bao, and Juyong Zhang. 2022. SelfRecon: Self Reconstruction Your Digital Avatar from Monocular Video. In *IEEE/CVF Conference on Computer Vision and Pattern Recognition (CVPR)*.

[30] Yoni Kasten, Dolev Ofri, Oliver Wang, and Tali Dekel. 2021. Layered neural atlases for consistent video editing. *ACM Transactions on Graphics (TOG)* 40, 6 (2021), 1–12.

[31] Hiroharu Kato, Yoshitaka Ushiku, and Tatsuya Harada. 2018. Neural 3D Mesh Renderer. In *The IEEE Conference on Computer Vision and Pattern Recognition (CVPR)*.

[32] Levon Khachatryan, Andranik Movsisyan, Vahram Tadevosyan, Roberto Henschel, Zhangyang Wang, Shant Navasardyan, and Humphrey Shi. 2023. Text2Video-Zero: Text-to-Image Diffusion Models are Zero-Shot Video Generators. *arXiv preprint arXiv:2303.13439* (2023).

[33] Yao-Chih Lee, Ji-Ze Genevieve Jang, Yi-Ting Chen, Elizabeth Qiu, and Jia-Bin Huang. 2023. Shape-aware Text-driven Layered Video Editing. arXiv:2301.13173 [cs.CV]

[34] Tingting Liao, Hongwei Yi, Yuliang Xiu, Jiaxiang Tang, Yangyi Huang, Justus Thies, and Michael J. Black. 2024. TADA! Text to Animatable Digital Avatars. In *International Conference on 3D Vision (3DV)*.

[35] Zhenyi Liao and Zhijie Deng. 2023. LOVECon: Text-driven Training-Free Long Video Editing with ControlNet. arXiv:2310.09711 [cs.CV]

[36] Jun Hao Liew, Hanshu Yan, Jianfeng Zhang, Zhongcong Xu, and Jiashi Feng. 2023. MagicEdit: High-Fidelity and Temporally Coherent Video Editing. In *arXiv*.

[37] Jing Lin, Ailing Zeng, Haoqian Wang, Lei Zhang, and Yu Li. 2023. One-Stage 3D Whole-Body Mesh Recovery with Component Aware Transformer. In *Proceedings of the IEEE/CVF Conference on Computer Vision and Pattern Recognition*. 21159–21168.

[38] Jia-Wei Liu, Yan-Pei Cao, Jay Zhangjie Wu, Weijia Mao, Yuchao Gu, Rui Zhao, Jussi Keppo, Ying Shan, and Mike Zheng Shou. 2023. DynVideo-E: Harnessing Dynamic NeRF for Large-Scale Motion- and View-Change Human-Centric Video Editing. *arXiv preprint arXiv:2310.10624* (2023).

[39] Shaoteng Liu, Yuechen Zhang, Wenbo Li, Zhe Lin, and Jiaya Jia. 2023. Video-P2P: Video Editing with Cross-attention Control.

[40] Wen Liu, Zhixin Piao, Min Jie, Wenhan Luo, Lin Ma, and Shenghua Gao. 2019. Liquid Warping GAN: A Unified Framework for Human Motion Imitation, Appearance Transfer and Novel View Synthesis. In *The IEEE International Conference on Computer Vision (ICCV)*.

[41] Wen Liu, Zhixin Piao, Zhi Tu, Wenhan Luo, Lin Ma, and Shenghua Gao. 2021. Liquid warping GAN with attention: A unified framework for human image synthesis. *IEEE Transactions on Pattern Analysis and Machine Intelligence* (2021).

[42] Zhengxiong Luo, Dayou Chen, Yingya Zhang, Yan Huang, Liang Wang, Yujun Shen, Deli Zhao, Jingren Zhou, and Tieniu Tan. 2023. VideoFusion: Decomposed Diffusion Models for High-Quality Video Generation. arXiv:2303.08320 [cs.CV]

[43] Aryan Mikaeili, Or Perel, Mehdi Safaee, Daniel Cohen-Or, and Ali Mahdavi-Amiri. 2023. SKED: Sketch-guided Text-based 3D Editing. *ICCV* (2023).

[44] Eyal Molad, Eliahu Horwitz, Dani Valevski, Alex Rav Acha, Yossi Matias, Yael Pritch, Yaniv Leviathan, and Yedid Hoshen. 2023. Dreamix: Video Diffusion Models are General Video Editors. arXiv:2302.01329 [cs.CV]

[45] Andrew Nealen, Takeo Igarashi, Olga Sorkine, and Marc Alexa. 2006. Laplacian Mesh Optimization. In *GRAPHITE*.

[46] Hao Ouyang, Qiuyu Wang, Yuxi Xiao, Qingyan Bai, Juntao Zhang, Kecheng Zheng, Xiaowei Zhou, Qifeng Chen, and Yujun Shen. 2023. CoDeF: Content Deformation Fields for Temporally Consistent Video Processing. *arXiv preprint arXiv:2308.07926* (2023).

[47] Georgios Pavlakos, Vasileios Choutas, Nima Ghorbani, Timo Bolkart, Ahmed A. A. Osman, Dimitrios Tzionas, and Michael J. Black. 2019. Expressive Body Capture: 3D Hands, Face, and Body from a Single Image. In *Proceedings IEEE Conf. on Computer Vision and Pattern Recognition (CVPR)*.

[48] Chenyang Qi, Xiaodong Cun, Yong Zhang, Chenyang Lei, Xintao Wang, Ying Shan, and Qifeng Chen. 2023. FateZero: Fusing Attentions for Zero-shot Text-based Video Editing. *arXiv:2303.09535* (2023).

[49] Bosheng Qin, Juncheng Li, Siliang Tang, Tat-Seng Chua, and Yueting Zhuang. 2023. InstructVid2Vid: Controllable Video Editing with Natural Language Instructions. arXiv:2305.12328 [cs.CV]

[50] Alec Radford, Jong Wook Kim, Chris Hallacy, Aditya Ramesh, Gabriel Goh, Sandhini Agarwal, Girish Sastry, Amanda Askell, Pamela Mishkin, Jack Clark,

Gretchen Krueger, and Ilya Sutskever. 2021. Learning Transferable Visual Models From Natural Language Supervision. *arXiv preprint arXiv:2103.00020* (2021).

[51] Ruizhi Shao, Jingxiang Sun, Cheng Peng, Zerong Zheng, Boyao Zhou, Hongwen Zhang, and Yebin Liu. 2024. Control4D: Efficient 4D Portrait Editing with Text. (2024).

[52] Uriel Singer, Adam Polyak, Thomas Hayes, Xi Yin, Jie An, Songyang Zhang, Qiyuan Hu, Harry Yang, Oron Ashual, Oran Gafni, Devi Parikh, Sonal Gupta, and Yaniv Taigman. 2022. Make-A-Video: Text-to-Video Generation without Text-Video Data. arXiv:2209.14792 [cs.CV]

[53] Wen Wang, kangyang Xie, Zide Liu, Hao Chen, Yue Cao, Xinlong Wang, and Chunhua Shen. 2023. Zero-Shot Video Editing Using Off-The-Shelf Image Diffusion Models. *arXiv preprint arXiv:2303.17599* (2023).

[54] Chung-Yi Weng, Brian Curless, Pratul P. Srinivasan, Jonathan T. Barron, and Ira Kemelmacher-Shlizerman. 2022. HumanNeRF: Free-Viewpoint Rendering of Moving People From Monocular Video. In *Proceedings of the IEEE/CVF Conference on Computer Vision and Pattern Recognition (CVPR)*. 16210–16220.

[55] Jay Zhangjie Wu, Yixiao Ge, Xintao Wang, Stan Weixian Lei, Yuchao Gu, Yufei Shi, Wynne Hsu, Ying Shan, Xiaohu Qie, and Mike Zheng Shou. 2023. Tune-a-video: One-shot tuning of image diffusion models for text-to-video generation. In *Proceedings of the IEEE/CVF International Conference on Computer Vision*. 7623–7633.

[56] Zhen Xing, Qi Dai, Han Hu, Zuxuan Wu, and Yu-Gang Jiang. 2023. SimDA: Simple Diffusion Adapter for Efficient Video Generation. *arXiv preprint arXiv:2308.09710* (2023).

[57] Zhongcong Xu, Jianfeng Zhang, Jun Hao Liew, Hanshu Yan, Jia-Wei Liu, Chenxu Zhang, Jiashi Feng, and Mike Zheng Shou. [n. d.]. MagicAnimate: Temporally Consistent Human Image Animation using Diffusion Model.

[58] Shuai Yang, Yifan Zhou, Ziwei Liu, , and Chen Change Loy. 2023. Rerender A Video: Zero-Shot Text-Guided Video-to-Video Translation. In *ACM SIGGRAPH Asia Conference Proceedings*.

[59] Shengming Yin, Chenfei Wu, Huan Yang, Jianfeng Wang, Xiaodong Wang, Minheng Ni, Zhengyuan Yang, Linjie Li, Shuguang Liu, Fan Yang, Jianlong Fu, Gong Ming, Lijuan Wang, Zicheng Liu, Houqiang Li, and Nan Duan. 2023. NUWA-XL: Diffusion over Diffusion for eXtremely Long Video Generation. arXiv:2303.12346 [cs.CV]

[60] David Junhao Zhang, Jay Zhangjie Wu, Jia-Wei Liu, Rui Zhao, Lingmin Ran, Yuchao Gu, Difei Gao, and Mike Zheng Shou. 2023. Show-1: Marrying Pixel and Latent Diffusion Models for Text-to-Video Generation. *arXiv preprint arXiv:2309.15818* (2023).

[61] Jianfeng Zhang, Hanshu Yan, Zhongcong Xu, Jiashi Feng, and Jun Hao Liew. 2023. MagicAvatar: Multi-modal Avatar Generation and Animation. In *arXiv*.

[62] Lvmin Zhang, Anyi Rao, and Maneesh Agrawala. [n. d.]. Adding Conditional Control to Text-to-Image Diffusion Models.

[63] Shangzhan Zhang, Sida Peng, Yinji ShenTu, Qing Shuai, Tianrun Chen, Kaicheng Yu, Hujun Bao, and Xiaowei Zhou. 2023. Dyn-E: Local Appearance Editing of Dynamic Neural Radiance Fields. arXiv:2307.12909 [cs.CV]

[64] Yabo Zhang, Yuxiang Wei, Dongsheng Jiang, Xiaopeng Zhang, Wangmeng Zuo, and Qi Tian. 2023. ControlVideo: Training-free Controllable Text-to-Video Generation. *arXiv preprint arXiv:2305.13077* (2023).

[65] Daquan Zhou, Weimin Wang, Hanshu Yan, Weiwei Lv, Yizhe Zhu, and Jiashi Feng. 2023. MagicVideo: Efficient Video Generation With Latent Diffusion Models. arXiv:2211.11018 [cs.CV]

[66] Qianshu Zhu, Chu Han, Guoqiang Han, Tien-Tsin Wong, and Shengfeng He. 2020. Video snapshot: Single image motion expansion via invertible motion embedding. *IEEE Transactions on Pattern Analysis and Machine Intelligence* 43, 12 (2020), 4491–4504.

[67] Shenhao Zhu, Junming Leo Chen, Zuozhuo Dai, Yinghui Xu, Xun Cao, Yao Yao, Hao Zhu, and Siyu Zhu. 2024. Champ: Controllable and Consistent Human Image Animation with 3D Parametric Guidance. In *European Conference on Computer Vision (ECCV)*.